An Approach of Irregular Porous Structure Modeling Based on Subdivision and NURBS

S. T. Kou[1] and S. T. Tan[2]

Department of Mechanical Engineering, The University of Hong Kong
[1] stkou@hku.hk
[2] sttan@hku.hk

ABSTRACT

Porous structure has its own unique advantages such as low relative density, high specific strength, high specific surface area and good permeability etc., and these advantages lead to porous structure's wide application in the field of rapid manufacturing, lightweight design and tissue engineering. Porous structure modeling, however, is a challenging task in CAD due to the difficulties in controlling the pore shape, size, diversity and interconnectivity. In this paper, we present a method for irregular porous structure modeling. Quadtree (Octree) is used to subdivide the modeling object into small sub-regions and the derived polygon (polyhedron) is generated in each of the sub-region. T-mesh is used in this paper as a refinement tool for subdivision. Finally non-uniform rational B-spline (NURBS) curves (surfaces) are generated using the derived polygon (polyhedron) as the control polygon (polyhedron). Easy control of the structure size and interconnectivity is achieved through the flexibility and independent characteristics of the quadtree (octree) structure and T-mesh. Structure irregularity is obtained by creating NURBS features based on the derived polygons or polyhedrons.

Keywords: porous structure modeling, subdivision, NURBS.
DOI: 10.3722/cadaps.2013.355-369

1 INTRODUCTION

Porous structure has low density, low thermal conductivity, low stiffness, high specific strength and high specific surface area [14], [27]. These properties and advantages enable porous structure being increasingly used in the field of rapid manufacturing, lightweight design and tissue engineering [13]. Several parameters are important in governing the properties of porous structure, namely pore size [9], [20, 21], [23], porosity [9], [36] and interconnectivity [9], [21, 22]. Other mechanical and transport properties can be derived from these parameters. The control of pore size, porosity and good

interconnectivity is the key element in porous structure design, and this has a direct relationship on the structure's performance.

There are mainly three kinds of porous structure modeling approaches, but none of them could satisfactorily fulfill the design requirements. For instance, the regular porous structure modeling method by performing repeated Boolean operations of the same unit cell or feature cannot guarantee pore diversity both in size and morphology; the 3D image reconstruction approach derived from reverse engineering needs an existing object at hand to mimic as a prerequisite [34].

This paper proposes a new representation of porous structure both in 2D and 3D which is more flexible and easier to control, where pore diversity is also guaranteed. In section 2, a brief literature review is presented and the research motivation is discussed. Section 3 presents an approach for object subdivision based on quadtree /octree representation [2] and an improvement is conducted by introducing T- mesh [8], [29]. Derived polygon and polyhedron are put forward in section 4 and porous structures are generated by NURBS curves and surfaces [25]. Both 2D and 3D case studies are implemented and illustrated. Discussions and conclusions are finally offered in section 5.

2 RELATED WORK AND MOTIVATIONS

2.1 Related Work

The study of porous structure first appeared in Robert Hooke's famous book *Micrographia* [40] where the natural porous structures in cork were recorded [17]. During the last decades, considerable approaches were put forward to model porous structure and these methods can be roughly classified into three categories, as shown in Fig. 1.

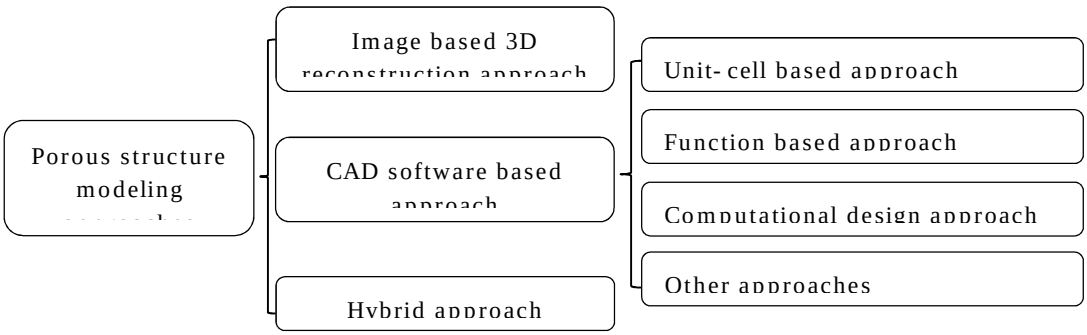

Fig. 1: Classification of porous structure design approaches.

Image based 3D reconstruction approach is widely used in biomedical research [34], [30]. The foundation of this approach is image modalities including computed tomography (CT), magnetic resonance imaging (MRI), optical microscopy and micro CT [33]. Applying these technologies, the existing porous object is scanned layer by layer and a 3D model is constructed in computer from the scanned 2D cross- sectional images after data processing. This method rebuilds the existing object at hand and mimics the porous structure in computer.

CAD software based approach doesn't need pre- existing objects and the modeling process is accomplished through computer software utilizing different theories and algorithms to represent the porous structure.

In unit-cell based approach, feature primitive represented with specific geometry is first built and porous structures are created through repeated Boolean operations of the feature primitive. The feature primitive is called unit cell and various unit cells form a library. The key issue here is how the unit cells are built to represent the desired structure and match the corresponding properties. Connie Gomez et al. [15] described the unit cell informatics and characterization. Sun et al. [33] designed a library of various unit cells by analogizing trabecular architectures found at different anatomical sites in the human skeleton. Chua et al. [6, 7] created a unit-cell library with eleven polyhedrons which are selected from Platonic solids, Archimedean solids, prisms and antiprisms. Wettergreen et al. [35] created a library containing two types of models, one is based on solid geometry with the inclusion of void spaces to create porosity and the other one is based on geometry of regular polyhedra. To overcome the stress discontinuities between two different unit cells, the concept of common interface is put forward.

In function based approach, the porous structure is described or controlled by functions. Yoo [37] and Gabbrielli et al. [12] proposed to represent porous structure using triply periodic minimal surfaces [39] which are those with zero mean curvature and a crystalline structure. Cai and Xi [3] introduced to use a shape function which is computed when making a transformation between two different coordinate systems. Irregular and deformed pore-making units are derived from regular basic units based on the shape function. Boolean difference is operated and irregular pores are removed from the solid. Pasko et al. [24] used different periodic functions for modeling porous structures within the Function Representation. These functions serve to directly define the structure shape.

In computational design approach, characteristics and properties related to the porous structure are formulated in a mathematical way so as to make a quantitative evaluation and prediction. Homogenization theory is commonly used in this approach especially in optimization design which uses asymptotic expansion of relevant physical variables to generate multiscale equilibrium equations to compute the effective properties [16]. Adachi et al. [1] built a model of scaffold degradation and new bone formation, and mechanical properties are formulated during the process. A three-dimensional computational simulation is conducted to evaluate the change of the mechanical properties and provides the desired function. Sanz-Herrera et al. [26] used a mathematical approach to study factors such as stiffness, porosity and pore size, and predicted in vivo the rate of bone formation, scaffold degradation and the interaction between implanted scaffold and the surrounding bone.

Inspired by random colloid-aggregation model, Kou and Tan [17] used Voronoi tessellation to partition a space into polygons and adjacent polygons with the same attributes are merged together. Closed B-spline curve is subsequently created in each polygon and porous structures are generated after Boolean difference between each polygon and its corresponding closed B-spline curve. Lal and Sun [18] constructed a three-dimensional microsphere-packed bone graft structure. Two extreme microsphere packing models and a statistical packing model are used to determine the number of spheres packed in a synthesized bone graft. Lian et al. [19] developed an approach to construct a 3D concentric microstructure through stacking a series of 2D concentric structures. Schroeder et al. [28] represented the model density and porosity based on stochastic geometry.

Some approaches are based on a mixture of the above methods. Approaches in [33] and [32] use 3D reconstruction approach to get the contour of the modeling object and subsequently unit cell based approach is applied to design the internal porous structure.

2.2 Motivations of this Research

Although many approaches have been proposed to model porous structure as is shown in the brief review above, no 'perfect' model is developed [31]. They mainly have the following disadvantages:

•A lack of pore diversity. A large proportion of existing approaches are for regular porous structures. Structures are usually built by repeated Boolean operations of the same unit cell. Characteristics such as pore architecture, pore size and porosity which have crucial influence on the mechanical properties and mass transportation are the same.

•Need of pre-existing objects and large memory storage. In image based 3D reconstruction approach, a pre-existing object should be available for scanning. A large amount of data is produced to represent the 3D object for reconstruction.

•Discontinuity in the overall structure. The unit cell based approach which is the most widely studied, collects the individual cells and assembles them together. Because the virtual structure is treated by the system as a collection of closely packed unit cells, discontinuity in the overall structure exists across the interface of individual unit cells throughout the entire volume of the scaffold [5]. This gives rise to weak mechanical properties in the joint between cells.

This paper puts forward an approach that can guarantee the flexible control and pore diversity of the structure. Requirements of pore size and distribution are achieved through flexible control. In the process, the domain is decomposed into smaller sub-regions. It is not formed from a collection of cells, thus no discontinuity problem arises.

3 SUBDIVISION

The proposed approach first subdivides the modeling domain into smaller sub-regions according to pore size and distribution. Quadtree (Octree) is used for the subdivision and T-mesh is utilized as a refinement tool.

3.1 Quadtree (Octree) Subdivision

Quadtree (Octree) is most often used to partition a two (three) dimensional space by recursively subdividing it into four (eight) quadrants and they are widely used in geometric modeling applications.

Given an object, an initial box S_0 is created to contain the domain entirely. It is then subdivided into four equal smaller boxes S_1. Any S_1 can be regarded as the initial box and further subdivision can be done on the sub-region. This procedure is repeated recursively. The area relationship between the initial box S_0 and the sub-regions after ith subdivision is

$$Aera_{S_i} = \frac{Aera_{S_0}}{2^{2i}}. \tag{1}$$

When the area of S_i is known, the subdivision times i can be calculated by

$$i = \frac{1}{2}\log_2 \frac{Aera_{S_0}}{Aera_{S_i}}. \tag{2}$$

Take the grassy stem [13] as an example, it is a hollow cylinder structure and the cross sections of the grassy stem are porous structures and the pores are denser and smaller near the outer boundary but sparser and larger in the inner boundary. The modeling process is illustrated in Fig. 2.

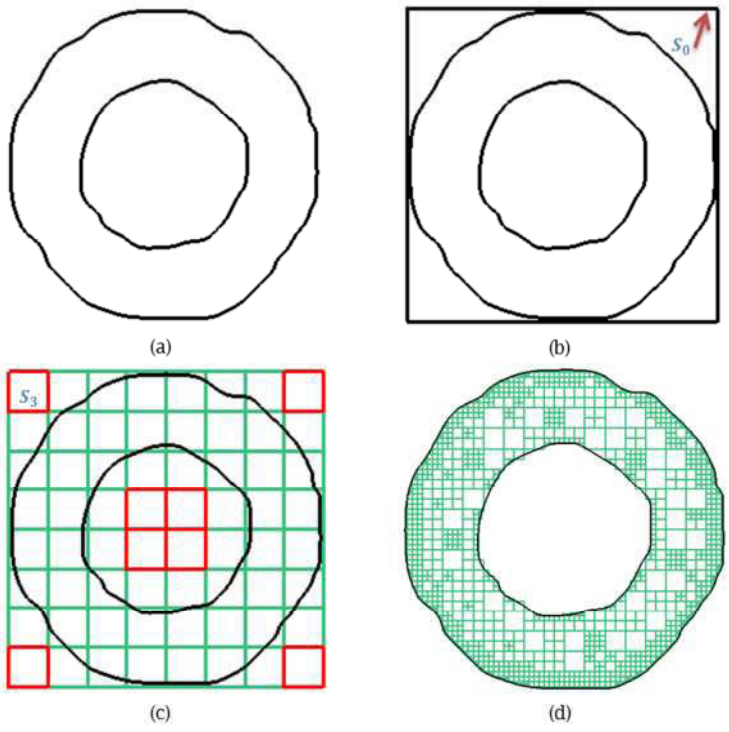

Fig. 2: Subdivision process (a) The domain (the contour of a cross section of the grassy stem) of the modeling object (b) S_0 is created to contain the domain entirely (c) After S_3 are created, red boxes need no subdivision and green ones will be subdivided further (d) Subdivision result based on pore size and distribution.

In 3D, octree tree subdivision is implemented and a cube is divided into eight sub- regions recursively, the subdivision times

$$i = \frac{1}{3}\log_2 \frac{Volume_{S_0}}{Volume_{S_i}}, \tag{3}$$

where $Volume_{S_0}$ is the volume of the initial cube S_0 and $Volume_{S_i}$ is the volume of the sub- regions after ith subdivision.

Quadtree (Octree) subdivision has the following unique advantages in porous structure modeling:

Flexibility- Pores contained in an object are usually not uniformly distributed and the pore size may vary. Quadtree (Octree) subdivision allows the object to be subdivided based on specified requirements. Areas with no pores such as the red boxes in Fig. 2 (c) need no further subdivision; on the contrary if pores are dense in S_i, further subdivision is needed.

Independence- Each sub- region is independent from the others that means the property is independent from each other, changes in one area will not affect the others. This is a useful 'handle' when one is doing modification to the design.

3.2 T-Meshes Subdivision

Inspired by T-splines [8], [29], T-mesh is used in this paper as a refinement tool for subdivision. T-mesh is a partition of a rectangle domain that allows T-junctions. When the domain is partitioned by quadtree, two partition lines divide the domain into four parts. T-mesh subdivision is more flexible because T-junctions allow the domain to be partitioned into two parts. In the grassy stem example, quadtree is implemented in Fig. 3 (b) and T-mesh is utilized in Fig. 3 (c) which is referred to as parametric T-mesh. Less redundant boxes are produced through T-mesh subdivision which leads to high efficiency and less memory storage.

Two parameters are used to define T-mesh, namely direction and percentage. Direction refers to the partition line as transverse or lengthways; percentage indicates the line's insertion location. Before implementing T-mesh, the two parameters are set as Fig. 4 shows.

A combination of quadtree and parametric T-mesh is seemingly a good compromised solution for specific cases and design requirements.

4 GENERATION OF POROUS STRUCTURES

After the modeling domain is subdivided into many sub-regions, porous structures are generated through NURBS. The concepts of 'derived polygon' and 'derived polyhedron' regarded as the control polygon and polyhedron of NURBS are utilized.

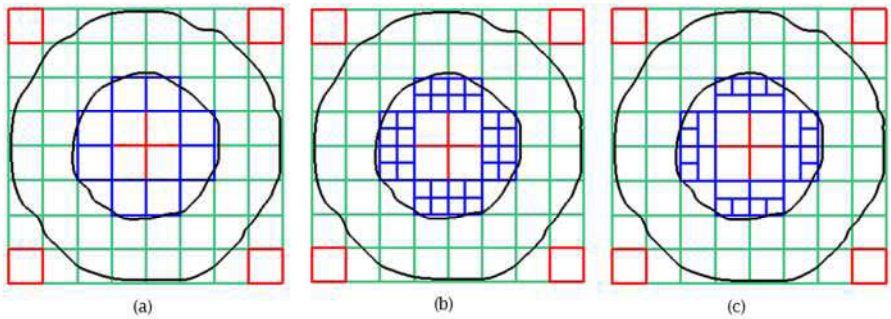

Fig. 3: Comparison of quadtree subdivision and T-mesh subdivision (a) the structure after three times subdivision (b) quadtree subdivision on blue boxes (c) T-mesh subdivision on blue boxes (boxes in red need no subdivision and further subdivision is done on blue ones for refinement).

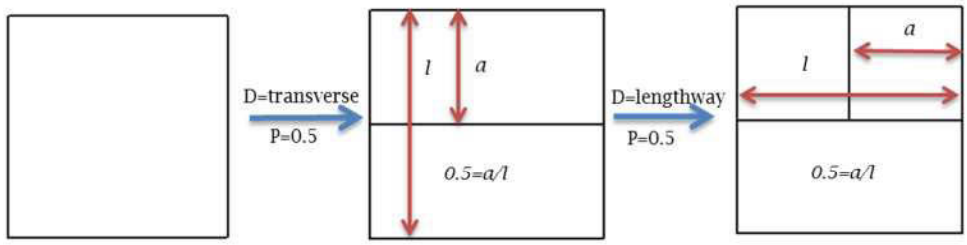

Fig. 4: Illustration of parametric T-mesh subdivision (D stands for direction and P stands for percentage).

4.1 2D Derived Polygon

Given a polygon with an even number of sides, the derived polygon is obtained by joining the points which are a fractional distance r along each side [38]. Derived hexagons are illustrated in Fig. 5 where $r = 0.5$.

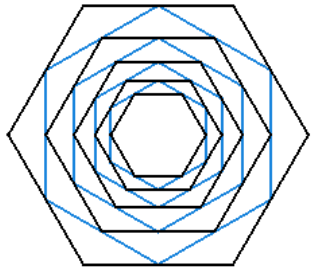

Fig. 5: Derived hexagons.

Inspired by the above idea, a derived polygon in this paper is defined by using different values of r in different edges(Fig. 6). The polygon $ABCD$ is called parent polygon and the new points A', B', C', D' are called derived points.

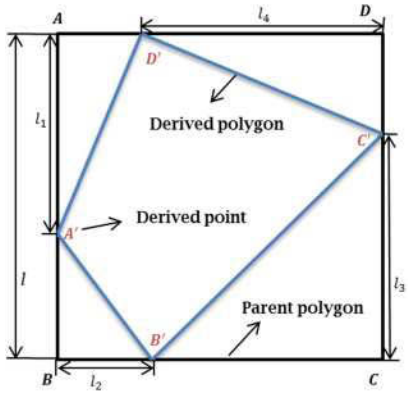

Fig. 6: Derived polygon (blue).

Area of the derived polygon in Fig. 6 $Area_{P_i}$ can be expressed as

$$Area_{P_i} = l^2 - 0.5 \times [l \cdot (l_1 + l_2 + l_3 + l_4) - (l_1 \cdot l_2 + l_2 \cdot l_3 + l_3 \cdot l_4 + l_4 \cdot l_1)] \quad (4)$$

Let $r_1 = \frac{l_1}{l}, r_2 = \frac{l_2}{l}, r_3 = \frac{l_3}{l}, r_4 = \frac{l_4}{l}$,

When

a. $r_1 = r_2 = r_3 = r_4 = 0$ *or* 1, the derived polygon is the parent polygon, $area = S_{max}$

b. $(r_1 = r_3 = 0$ *and* $r_2 = r_4 = 1)$ *or* $(r_1 = r_3 = 1$ *and* $r_2 = r_4 = 0)$, the derived polygon disappears and $area = 0$

Using this derived polygon concept, a NUBRS curve is generated (Fig. 7 (a)). Knots and weights are set with reference to [41]. The area enclosed by the NURBS curve is subtracted by Boolean difference and a pore within a sub- region is created (Fig. 7 (b)).

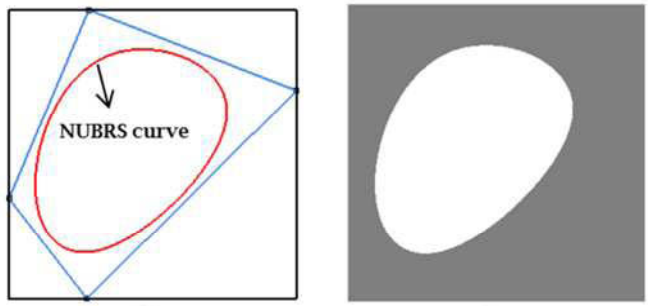

Fig. 7: 2D porous structure.

The porosity of the 2D porous structure can be formulized as

$$P = \frac{Area_{N_i}}{Area_{S_i}}, \tag{5}$$

$$Area_{N_i} = \alpha Area_{P_i}, \tag{6}$$

where $Area_{N_i}$ is the area enclosed by the NURBS curve and α is the ratio of $Area_{N_i}$ to $Area_{P_i}$.

If porosity P is a known parameter, from equation (4)- (6) we can get

$$l \cdot (l_1 + l_2 + l_3 + l_4) - (l_1 \cdot l_2 + l_2 \cdot l_3 + l_3 \cdot l_4 + l_4 \cdot l_1) = 2\left(l^2 - \frac{P \cdot Area_{S_i}}{\alpha}\right) = \beta, \tag{7}$$

where β is a constant.

If three of the four parameters l_1, l_2, l_3, l_4 are known, the fourth one can be derived

$$l_4 = \frac{\beta + l_1 \cdot l_2 + l_2 \cdot l_3 - l \cdot (l_1 + l_2 + l_3)}{l - l_1 - l_3}. \tag{8}$$

When the order of NURBS curve is 3, α is approximately equal to 0.83 according to large experiments data.

4.2 3D Derived Polyhedron

Derived polyhedron is referred to as the control polyhedron of the NURBS pore which will be subtracted from the sub- region. In 3D, each vertex of a box is the intersection of three faces and according to the definition of derived polygon, each vertex has three derived points on the three intersected faces as illustrated in Fig. 8 (a). Thus given a box whose vertices are $A, B, \ldots, H$, the derived polyhedron is obtained by joining new vertices, and each new vertex (A') is related with the corresponding derived points (A_1, A_2 *and* A_3). The given box is called parent polyhedron and its vertices ($A, B, \ldots, H$) are parent vertices.

Inspired by the subdivision modeling methods of 'Doo- Sabin' [10, 11] and 'Catmull- Clark' [4] that smooth the surface by generating new points based on the old points, edges or surfaces, we propose an approach to generate new vertex A' from its parent vertex A and the three derived points A_1, A_2, A_3. These four points form a tetrahedron (see Fig. 8(b)) and the new vertex A' is the centroid,

$$A' = \frac{1}{4}(A + A_1 + A_2 + A_3). \tag{9}$$

The eight new vertices form the derived polyhedron which is regarded as the control polyhedron of the NURSB pore.

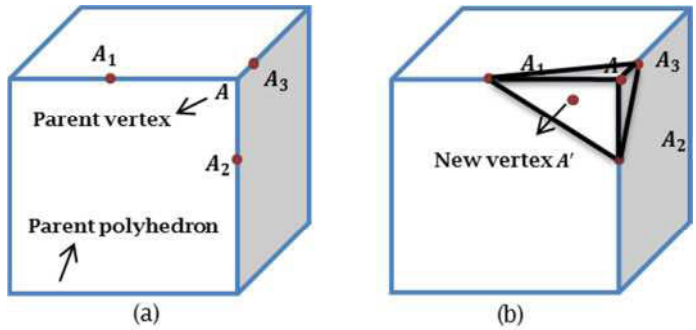

Fig. 8: Illustration of 3D derived polyhedron.

As an example in Fig. 9, the blue points are the new vertices and the red solid is the NURBS pore obtained from the derived polyhedron. The porosity of the 3D porous structure

$$P = \frac{Volume_{N_i}}{Volume_{S_i}}. \tag{10}$$

In Eq. (9), A' is determined by $A, A_1, A_2 and\ A_3$ where $A_1, A_2 and\ A_3$ are changeable. Parameter t is used to describe the location of each derived point. When $A_1, A_2 and\ A_3$ are the coincident points of A, the pore and porosity is maximum and under the circumstances $t = 0$; when $A_1, A_2 and\ A_3$ are the points of the other parent vertices of their corresponding edges, the pore and porosity is minimum and under the circumstances $t = 1$.

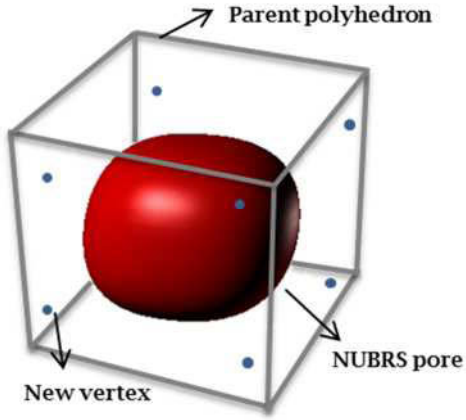

Fig. 9: A NURBS pore based on the derived polyhedron.

Boolean difference is operated between the NURBS pore and the sub- region after octree subdivision. In order to guarantee the interconnectivity of the porous structure, the parent polyhedron should be larger than the sub- region. The value range of parameter t is set so as that the pore is tangent to the sub- region's faces when t is minimal (see Fig. 10(a)), and the porosity is also minimal $P = 52.36\%$; the

pore is tangent to the sub-region's edges when t is maximal (see Fig. 10(b)), and the porosity has the maximal value $P = 96.5\%$. Any pore between the maximum and minimum is bound to have intersections with the sub-region results in a 3D irregular porous structure as shown in Fig. 11 and the porosity $52.36\% < P < 96.5\%$.

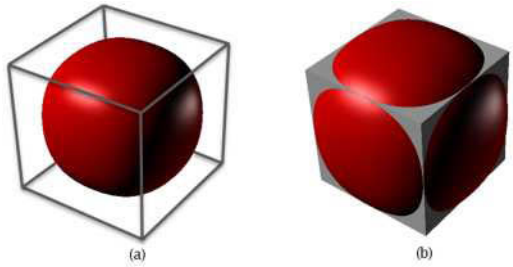

Fig. 10: The minimal and maximal pores of a sub-region.

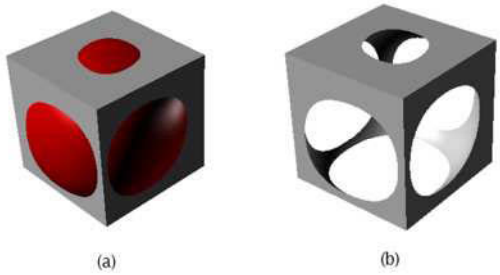

Fig. 11: 3D irregular porous structures.

4.3 Case Studies

Fig. 12 shows structures with different porosities modeled by methods in section 4.1. By applying this approach, accurate porosites can be achieved and controlled and at the same time, the pores' size is also under control by quadtree subdivision. The 2D porous structure generation is implemented on the grassy stem tubular structure as Fig. 13 illustrated. The outer cylinder shell is composed of dense cells surrounding the elliptical-liked pores, and the central region is hollow. The subdivision times are different in different regions according to the pore size. Assume the average pore size is m in the outer side and n in the inner part, the subdidvision time $i = \frac{1}{2}\log_2 \frac{Aera_{S_0}}{Aera_{S_i}}, Aera_{S_i} = \frac{m}{P}$ *or* $\frac{n}{P}$.

An example of 3D porous structure modeling is illustrated in Fig. 14 and a real object is manufactured by Rapid Prototyping in Fig. 15. It is a bone-shaped porous structure containing more than 1000 pores and the modeling time is about 4.5 minutes. 3D porous objects made by approach in section 4.2 can guarantee the interconnectivity well and control the pore size through octree subdivision, while the precise control of porosity is not easily obtained. The porosity is controlled by the eight new vertices and each new vertex is determined by another four points (three are changeable and one is fixed), in another word each new vertex is determined by three parameters. It may cost large computation and spend lots of time and storage. A preferable way to control the porosity roughly is to set the parameters through experiment data.

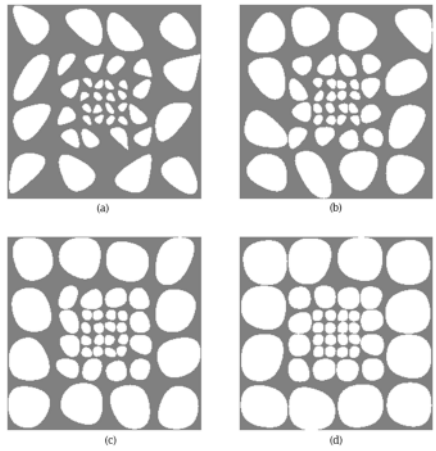

Fig. 12: 2D porous structures with different porosities, (a) 40%, (b) 50%, (c) 60%, (d) 70%.

Fig. 13: Model of the grassy stem.

5 DISCUSSIONS AND CONCLUSIONS

A new approach based on quadtree (octree) and T- mesh for representing porous structures is proposed in this paper. Pore distribution is guaranteed by the flexibility of the quadtree and octree. T-mesh is applied as a useful tool to improve the subdivision efficiency. Derived polygon and polyhedron are introduced as the control polygon and polyhedron to generate NURBS curve and surface. The polygon and polyhedron are controlled by the parameters that have direct relations with pore area and shape. This at one hand guarantees the control ability to pore properties; on the other hand the diversity is achieved by setting different values of the parameters. Authors of [17] also use subdivision approach and Voronoi Diagram is applied; in this paper quadtree (octree) is used to do so due to its unique advantages. This paper also introduces the porous structure modeling approach in 3D case while paper [17] mainly focuses in 2D.

In this paper, several parameters are defined to modify the porous structure and they can be set by the users manually or can also be generated by the system randomly. These parameters describe the porous structure roughly and quantitative relationship between the parameters and the desired properties such as the mechanical strength are still not clear and further research needs to be done.

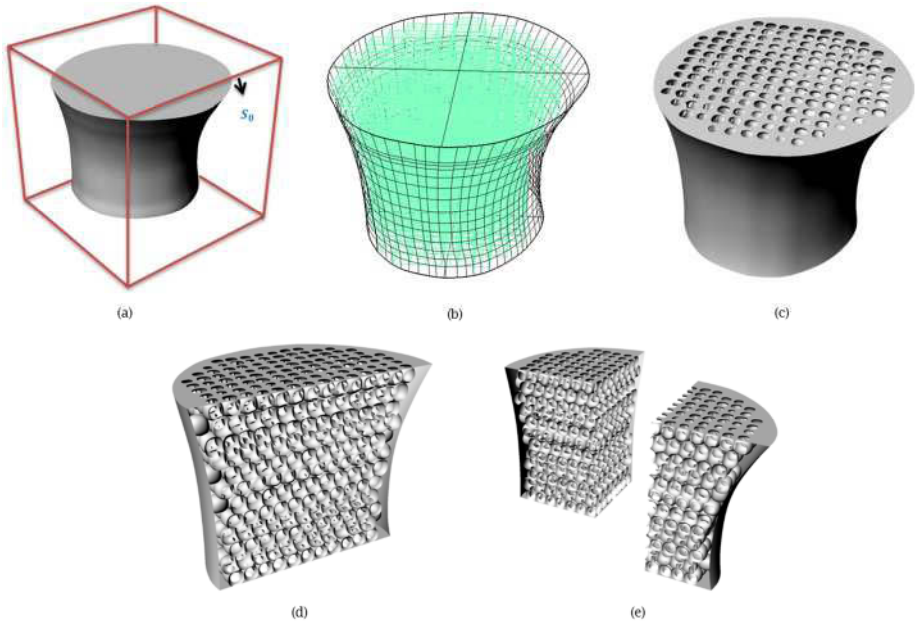

Fig. 14: A bone shaped porous structures model (a) S_0 is generated to contain the modeling object (b) Object after subdivision (the green boxes are the sub-regions after octree subdivision) (c) Porous structures after implemented the algorithm in 4.2 (d)(e) Sectional view of the porous structures.

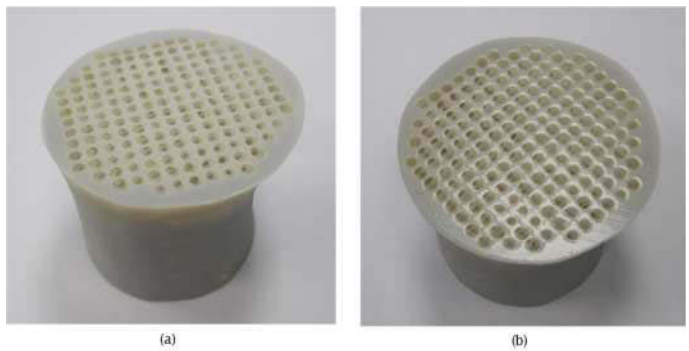

Fig. 15: Model made by Rapid Prototyping.

6 ACKNOWLEDGENTS

The authors would like to thank the Department of Mechanical Engineering, the University of Hong Kong and the Research Grant Council of Hong Kong SAR Government for supporting this project. The authors also would like to thank Dr. X. Y. Kou for his valuable comments, suggestions and corrections.

REFERENCES

[1] Adachi, T.; Osako, Y.; Tanaka, M.; Hojo, M.; Hollister, S. J.: Framework for optimal design of porous scaffold microstructure by computational simulation of bone regeneration, Biomaterials, 27(21), 2006, 3964-3972. DOI: 10.1016/j.biomaterials.2006.02.039

[2] Berg, M. D.; Cheong, O.; Kreveld, M. V.; Overmars, M.: Computational Geometry: Algorithms and Applications, Third Edition, Springer, 2008.

[3] Cai, S.; Xi, J.: A control approach for pore size distribution in the bone scaffold based on the hexahedral mesh refinement, Computer Aided Design, 40(10-11), 2008, 1040-1050. DOI: 1016/j.cad.2008.09.004

[4] Catmull, E.; Clark, J.: Recursively generated B-spline surfaces on arbitrary topological meshes, Computer-Aided Design, 10(6), 1978, 350-355. DOI: 10.1016/0010-4485(78)90110-0

[5] Cheah, C. M.; Chua, C. K.; Leong, K. F.; Cheong, C. H.; Naing, M. W.: Automatic Algorithm for Generating Complex Polyhedral Scaffold Structures for Tissue Engineering, Tissue Engineering, 10(3-4), 2004, 595-610. DOI: 10.1089/107632704323061951

[6] Chua, C. K.; Leong, K. F.; Cheah, C. M.; Chua, S. W.: Development of a tissue engineering scaffold structure library for rapid prototyping. Part 1: Investigation and classification, International Journal of Advanced Manufacturing Technology, 21(4), 2003, 291-301. DOI: 10.1007/s001700300034

[7] Chua, C. K.; Leong, K. F.; Cheah, C. M.; Chua, S. W.: Development of a tissue engineering scaffold structure library for rapid prototyping. Part 2: Parametric library and assembly program, International Journal of Advanced Manufacturing Technology, 21(4), 2003, 302-312. DOI: 10.1007/s001700300035

[8] Deng, J.; Chen, F.; Li, X.; Hu, C.; Tong, W.; Yang, Z.; Feng, Y.: Polynomial splines over hierarchical T-meshes, Graphical Models, 70(4), 2008, 76-86. DOI: 10.1016/j.gmod.2008.03.001

[9] Diego, R. B.; Esteîlés, J. M.; Sanz, J. A.; García-Asnar, J. M.; Sánchez, M. S.: Polymer scaffolds with interconnected spherical pores and controlled architecture for tissue engineering: Fabrication, mechanical properties, and finite element modeling, Journal of Biomedical Materials Research - Part B Applied Biomaterials, 81(2), 2007, 448-455. DOI: 10.1002/jbm.b.30683

[10] Doo, D.: A subdivision algorithm for smoothing down irregularly shaped polyhedrons, Paper presented at the Proceedings on Interactive Techniques in Computer Aided Design, Bologna, Italy, 1978.

[11] Doo, D.; Sabin, M.: Behaviour of recursive division surfaces near extraordinary points, Computer-Aided Design, 10(6), 1978, 356-360. DOI: 10.1016/0010-4485(78)90111-2

[12] Gabbrielli, R.; Turner, I. G.; Bowen, C. R.: Development of modelling methods for materials to be used as bone substitutes, Key Engineering Materials, 361 - 363, 2008, 903-906.

[13] Gibson, L. J.: Biomechanics of cellular solids, Journal of Biomechanics, 38(3), 2005, 377-399. DOI: 10.1016/j.jbiomech.2004.09.027

[14] Gibson, L. J.; Ashby, M. F.: Cellular solids: structure and properties, Cambridge University Press, 1997.

[15] Gomez, C.; Shokoufandeh, A.; Sun, W.: Unit-cell based design and modeling in tissue engineering applications, Computer-Aided Design and Applications, 4(1-6), 2007, 649-659.

[16] Hollister, S. J.: Porous scaffold design for tissue engineering, Nature Materials, 4, 2005, 518 - 524. DOI: 10.1038/nmat1421

[17] Kou, X. Y.; Tan, S. T.: A simple and effective geometric representation for irregular porous structure modeling, Computer Aided Design, 42(10), 2010, 930-941. DOI: 10.1016/j.cad.2010.06.006

[18] Lal, P.; Sun, W.: Computer modeling approach for microsphere-packed bone scaffold, Computer Aided Design, 36(5), 2004, 487-497. DOI: 10.1016/S0010-4485(03)00134-9

[19] Lian, Q.; Li, D. C.; Tang, Y. P.; Zhang, Y. R.: Computer modeling approach for a novel internal architecture of artificial bone, Computer Aided Design, 38(5), 2006, 507-514. DOI: 10.1016/j.cad.2005.12.001

[20] Ma, P. X.; Choi, J. W.: Biodegradable polymer scaffolds with well-defined interconnected spherical pore network, Tissue Engineering, 7(1), 2001, 23-33. DOI: 10.1089/107632701300003269

[21] Melchels, F. P. W.; Tonnarelli, B.; Olivares, A. L.; Martin, I.; Lacroix, D.; Feijen, J.; Grijpma, D. W.: The influence of the scaffold design on the distribution of adhering cells after perfusion cell seeding, Biomaterials, 32(11), 2011, 2878-2884. DOI: 10.1016/j.biomaterials.2011.01.023

[22] Miot, S.; Woodfield, T.; Daniels, A. U.; Suetterlin, R.; Peterschmitt, I.; Heberer, M.; Martin, I.: Effects of scaffold composition and architecture on human nasal chondrocyte redifferentiation and cartilaginous matrix deposition, Biomaterials, 26(15), 2005, 2479-2489. DOI: 10.1016/j.biomaterials.2004.06.048

[23] Nandiyanto, A. B. D.; Hagura, N.; Iskandar, F.; Okuyama, K.: Design of a highly ordered and uniform porous structure with multisized pores in film and particle forms using a template-driven self-assembly technique, Acta Materialia, 58(1), 2010, 282-289. DOI: 10.1016/j.actamat.2009.09.004

[24] Pasko, A.; Vilbrandt, T.; Fryazinov, O.; Adzhiev, V.: Procedural function-based spatial microstructures, 2010. DOI: 10.1109/SMI.2010.19

[25] Piegl, L.; Tiller, W.: The NURBS book, Springer, 1997.

[26] Sanz-Herrera, J. A.; García-Aznar, J. M.; Doblaré, M.: On scaffold designing for bone regeneration: A computational multiscale approach, Acta Biomaterialia, 5(1), 2009, 219-229. DOI: 10.1016/j.actbio.2008.06.021

[27] Scheffler, M.; Colombo, P.: Cellular ceramics : structure, manufacturing, properties and applications: Weinheim : Wiley-VCH, 2005.

[28] Schroeder, C.; Regli, W. C.; Shokoufandeh, A.; Sun, W.: Computer-aided design of porous artifacts, Computer Aided Design, 37(3), 2005, 339-353. DOI: 10.1016/j.cad.2004.03.008

[29] Sederberg, T. W.; Zheng, J.; Bakenov, A.; Nasri, A.: T-splines and T-NURCCs, ACM Transaction on Graphics, 22(3), 2003, 477-484. DOI: 10.1145/882262.882295

[30] Starly, B.; Fang, Z.; Sun, W.; Shokoufandeh, A.; Regli, W.: Three-dimensional reconstruction for medical-CAD modeling, Computer-Aided Design and Applications, 2(1-4), 2005, 431-438.

[31] Sun, W.; Darling, A.; Starly, B.; Nam, J.: Computer-aided tissue engineering: Overview, scope and challenges. Biotechnology and Applied Biochemistry, 39(1), 2004, 29-47.

[32] Sun, W.; Starly, B.; Darling, A.; Gomez, C.: Computer-aided tissue engineering: Application to biomimetic modelling and design of tissue scaffolds. Biotechnology and Applied Biochemistry, 39(1), 2004, 49-58.

[33] Sun, W.; Starly, B.; Nam, J.; Darling, A.: Bio-CAD modeling and its applications in computer-aided tissue engineering, Computer Aided Design, 37(11), 2005, 1097-1114. DOI: 10.1016/j.cad.2005.02.002

[34] Vergés, E.; Ayala, D.; Grau, S.; Tost, D.: 3D reconstruction and quantification of porous structures. Computers and Graphics (Pergamon), 32(4), 2008, 438-444. DOI: 10.1016/j.cag.2008.04.001

[35] Wettergreen, M. A.; Bucklen, B. S.; Starly, B.; Yuksel, E.; Sun, W.; Liebschner, M. A. K.: Creation of a unit block library of architectures for use in assembled scaffold engineering, Computer Aided Design, 37(11), 2005, 1141-1149. DOI: 10.1016/j.cad.2005.02.005

[36] Woodard, J. R.; Hilldore, A. J.; Lan, S. K.; Park, C. J.; Morgan, A. W.; Eurell, J. A. C.; Wagoner Johnson, A. J.: The mechanical properties and osteoconductivity of hydroxyapatite bone

scaffolds with multi-scale porosity. Biomaterials, 28(1), 2007, 45-54. DOI: 10.1016/j.biomaterials.2006.08.021

[37] Yoo, D. J.: Computer-aided porous scaffold design for tissue engineering using triply periodic minimal surfaces. International Journal of Precision Engineering and Manufacturing, 12(1), 2001, 61-71. DOI: 10.1007/s12541-011-0008-9

[38] http://mathworld.wolfram.com/DerivedPolygon.html

[39] http://www.susqu.edu/brakke/evolver/examples/periodic/periodic.html

[40] http://archive.nlm.nih.gov/proj/ttp/flash/hooke/hooke.html

[41] http://www.mactech.com/articles/develop/issue_25/schneider.html